PERGAMON

Computers & Fluids 32 (2003) 59–71

computers & fluids

www.elsevier.com/locate/compfluid

An arbitrary Lagrangian Eulerian formulation for residual distribution schemes on moving grids

C. Michler [*,1], H. De Sterck, H. Deconinck

von Karman Institute for Fluid Dynamics, Waterloose Steenweg 72, 1640 Sint-Genesius-Rode, Belgium

Accepted 26 June 2001

Abstract

The arbitrary Lagrangian Eulerian formulation is derived for the residual distribution method on moving meshes. The system of Euler equations is discretized on moving meshes and in case of deforming meshes a geometrical source term has to be taken into account. A conservative linearization guarantees the conservation property of the discretized equations.

From the geometric conservation law we obtain the appropriate integration points in time for the cell fluctuation and a guideline for how to distribute the geometrical source term.

Testcases include the flow around a transonic oscillating airfoil and a convected vortex. In the first case a rigidly moving mesh is employed, while in the other testcase a deforming mesh is used to investigate the influence of the geometrical source term on the solution.

Keywords: Residual distribution schemes; Arbitrary Lagrangian Eulerian formulation; Moving meshes; Geometric conservation law; Conservative linearization

1. Introduction

In many modern computational fluid dynamics applications, the fluid domain is enclosed by moving boundaries. It then becomes necessary to solve the time-dependent governing equations on a moving mesh (see [1–4]).

* Corresponding author.

E-mail addresses: c.michler@lr.tudelft.nl (C. Michler), desterck@vki.ac.be (H. De Sterck), deconinck@vki.ac.be (H. Deconinck).

[1] Present address: Faculty of Aerospace Engineering, Delft University of Technology, P.O. Box 5058, 2600 GB Delft, The Netherlands.

0045-7930/03/$ - see front matter
PII: S0045-7930(01)00095-0

In this work, we present theoretical considerations for flow computations on moving meshes using the residual distribution technique which has emerged in recent years as an alternative to the more well-known finite volume and finite element techniques (see [5–8]). We derive a formulation for the system of Euler equations within the framework of an arbitrary Lagrangian Eulerian (ALE) methodology. For unsteady flow computations on dynamic meshes, i.e. rigidly moving as well as deforming meshes, it seems logical to choose an ALE scheme that preserves the trivial solution of a uniform flow field. Indeed, it turns out that an additional conservation law, the so-called Geometric Conservation Law (GCL) has to be fulfilled. A conservative linearization is applied to evaluate the different integrals of the cell fluctuation which results in different expressions for the ALE formulation than for a fixed domain.

In Section 2, we briefly recall the basics of residual distribution schemes. Next, we derive the ALE formulation and the conditions imposed by the GCL. The GCL gives a guideline for evaluating geometrical quantities including the grid position and velocity. Further, it determines how the geometrical source term which arises in the ALE formulation for deforming meshes has to be distributed.

In Section 4, we compute the flow around a transonic oscillating airfoil on a rigidly moving mesh. In Section 5, we investigate the influence of the geometrical source term in the testcase of a convected vortex on a deforming mesh.

2. Theory for residual distribution schemes on fixed triangular meshes

In two dimensions, the system of Euler equations reads

$$\frac{\partial U}{\partial t}+\frac{\partial F}{\partial x}+\frac{\partial G}{\partial y}=0, \tag{1}$$

where $U=(\rho,\ \rho u,\ \rho v,\ \rho E)^{\tau}$ is the vector of conserved variables and $F=(\rho u,\ \rho u^2+p,\ \rho uv,\ \rho uH)^{\tau}$ and $G=(\rho v,\ \rho uv,\ \rho v^2+p,\ \rho vH)^{\tau}$ are the inviscid fluxes. The system is closed by the state equation for a perfect gas. We use capital letters as U, F, G to refer to arrays composed of the different terms of the equation system, whereas we will use the $\vec{}$ symbol or the $_k$ in index notation to indicate vectors in space.

In the residual distribution method, also known as the fluctuation splitting method, the solution is approximated continuously over the elements by piecewise linear (P1) shape functions. The cell fluctuation Φ^T is defined as

$$\Phi^T=-\int_{S_T}\frac{\partial U}{\partial t}\,\mathrm{d}\Omega=\int_{S_T}\left(\frac{\partial F}{\partial x}+\frac{\partial G}{\partial y}\right)\mathrm{d}\Omega, \tag{2}$$

where S_T denotes the cell area of a triangle. The nodal residual R_i is then computed by redistributing (splitting) the fluctuation to the vertices of the cell by the matrix of distribution coefficients $|\mathbf{B}_i$, with the summation extending over all triangles surrounding node i:

$$R_i=\sum_T|\mathbf{B}_i^T\Phi^T=\sum_T\Phi_i^T. \tag{3}$$

For consistency the $|\mathbf{B}_i^T$ must sum up to the identity matrix within an element.

The equivalence of the finite element Petrov–Galerkin formulation with the spatial discretization of the residual distribution approach can be found in [9]. In the present work we use Galerkin weighting functions for the discretization of the time derivative while using different weighting functions for the spatial discretization, which is called an inconsistent formulation. The elements of the mass matrix are defined as

$$m_{ij}^{T} = \frac{1}{S_T} \int_{S_T} \omega_i N_j \, \mathrm{d}\Omega, \tag{4}$$

where N_j denotes the shape function and ω_i the weighting function. We obtain the inconsistent lumped mass matrix by lumping the elements of each row to the diagonal:

$$\left[m_{ij}^{\mathrm{L,inc},T}\right] = \tfrac{1}{3} I \tag{5}$$

with identity matrix I. The assembling procedure of the inconsistent lumped mass matrix multiplied by the cell area S_T yields the median dual cell area S_i. Using the Einstein summation convention we write

$$\sum_T m_{ij}^{\mathrm{L,inc},T} S_T \frac{\mathrm{d}U_j}{\mathrm{d}t} + \sum_T |\mathbf{B}_i^T \Phi^T = S_i \frac{\mathrm{d}}{\mathrm{d}t}(U_i) + \sum_T \Phi_i^T = 0. \tag{6}$$

We use explicit Euler time integration with inconsistent lumped mass matrix and the PSI- or LDA-scheme for the space discretization [7]. The update for node i is then given by

$$U_i^{n+1} = U_i^n - \frac{\Delta t}{S_i} \sum_T \Phi_i^T. \tag{7}$$

This leads to first-order accurate schemes in space and time. Second-order accurate schemes are still under development (see [5,9,10]) and not yet mature enough to do ALE computations with residual distribution schemes.

3. Theoretical considerations for flow computations on moving meshes

3.1. ALE formulation

We consider a system of conservation laws written in an Eulerian frame:

$$\frac{\partial U}{\partial t} + \vec{\nabla} \cdot \vec{F} = 0, \tag{8}$$

where $\vec{F} = (F, G)$ denotes the vector of inviscid fluxes.

The formulation on a moving domain $\Omega(t)$ is derived by applying the Leibniz and Gauss theorems. For a control volume moving with an arbitrary speed $\vec{b}$, it reads

$$\frac{\mathrm{d}}{\mathrm{d}t} \int_{\Omega(t)} U \, \mathrm{d}\Omega + \int_{\Omega(t)} \vec{\nabla} \cdot (\vec{F} - U\vec{b}) \, \mathrm{d}\Omega = 0. \tag{9}$$

Eq. (9) is then discretized in time as

$$\sum_T m_{ij}^T \frac{\mathrm{d}}{\mathrm{d}t}(U_j S_T) + \sum_T \int_{S_T} \omega_i \frac{\partial}{\partial x_k}(F_k - U b_k)\,\mathrm{d}\Omega = 0 \tag{10}$$

with m_{ij}^T denoting the mass matrix. For deforming meshes the element area S_T changes in time and therefore has to be inside the time derivative.

3.2. Derivation of the GCL and its requirements

It is crucial to establish where the fluxes must be integrated: on the mesh configuration at $t = t^n$ (i.e. at grid position x^n), on that at $t = t^{n+1}$ (at grid position x^{n+1}), or in between these two configurations. The same questions arise for the choice of the mesh velocity vector. A logical requirement is that a numerical algorithm conserves the state of a uniform flow on a dynamic mesh. This requirement is the GCL.

We consider Eq. (10) and split the second term in two parts

$$\sum_T m_{ij}^T \frac{\mathrm{d}}{\mathrm{d}t}(U_j S_T) + \sum_T \int_{S_T} \omega_i \left(\frac{\partial F_k}{\partial x_k} - \frac{\partial U}{\partial x_k} b_k \right) \mathrm{d}\Omega - \sum_T \int_{S_T} \omega_i \frac{\partial b_k}{\partial x_k} U\,\mathrm{d}\Omega = 0. \tag{11}$$

The last term in Eq. (11) which is proportional to the divergence of the grid velocity represents a geometrical source term arising for deformable meshes. For rigidly moving meshes this term is zero. Using the finite element discretization $U = N_j U_j$ for the source term and Eq. (4) for the mass matrix m_{ij}^T allows rewriting Eq. (11) as

$$\sum_T m_{ij}^T \frac{\mathrm{d}}{\mathrm{d}t}(U_j S_T) + \sum_T \int_{S_T} \omega_i \left(\frac{\partial F_k}{\partial x_k} - \frac{\partial U}{\partial x_k} b_k \right) \mathrm{d}\Omega - \sum_T m_{ij}^T \frac{\partial b_k}{\partial x_k} U_j S_T = 0. \tag{12}$$

The GCL requires that the trivial solution of a uniform flow is preserved on a dynamic mesh. Considering Eq. (12) for a uniform flow, i.e. $U = U_j = \text{constant}$, the second term vanishes. For the other two terms $U_j = \text{constant}$ cancels out and we rewrite Eq. (12) as

$$\sum_T m_{ij}^T \frac{\mathrm{d}}{\mathrm{d}t} S_T - \sum_T m_{ij}^T \frac{\partial b_k}{\partial x_k} S_T = \sum_T m_{ij}^T \left(\frac{\mathrm{d}}{\mathrm{d}t} S_T - \frac{\partial b_k}{\partial x_k} \int_{S_T} \mathrm{d}\Omega \right) = 0. \tag{13}$$

From Eq. (13), it becomes apparent that the source term has to be treated in the same way as the time derivative if we want to satisfy the GCL. This implies that for Galerkin weighting functions and a lumped mass matrix we have to distribute it equally to the nodes by $\frac{1}{3}$. Furthermore, for a consistent mass matrix the source term has to be distributed with the same consistent mass matrix. In the following, we derive the GCL for a general mass matrix.

Considering Eq. (13) for a spatially linearly varying b_k gives

$$\frac{\mathrm{d}}{\mathrm{d}t} S_T - \int_{S_T} \frac{\partial b_k}{\partial x_k}\,\mathrm{d}\Omega = 0, \tag{14}$$

since then $\partial b_k / \partial x_k = \text{constant}$. Time integration of Eq. (14) gives

$$S_T^{n+1} - S_T^n = \int_{t^n}^{t^{n+1}} \int_{S_T} \vec{\nabla} \cdot \vec{b}\,\mathrm{d}\Omega\,\mathrm{d}t = \int_{t^n}^{t^{n+1}} \int_{\partial S_T} \vec{b} \cdot \vec{n}\,\mathrm{d}\Gamma\,\mathrm{d}t. \tag{15}$$

Eq. (15) defines a GCL that must be satisfied by the ALE mesh updating scheme. This requirement imposes that the change in area of each cell between t^n and t^{n+1} must be equal to the area swept by the cell boundary during $\Delta t = t^{n+1} - t^n$. From the analysis presented above, it follows that an appropriate scheme for evaluating $\int_{t^n}^{t^{n+1}} \int_{S_T} \frac{\partial}{\partial x_k}(F_k - Ub_k)\,\mathrm{d}\Omega\,\mathrm{d}t = \int_{t^n}^{t^{n+1}} \Phi^T\,\mathrm{d}t$ is a scheme that respects the GCL (15) and therefore computes exactly the right hand side of Eq. (15)-that is $\int_{t^n}^{t^{n+1}} \int_{\partial S_T} \vec{b}\cdot\vec{n}\,\mathrm{d}\Gamma\,\mathrm{d}t$.

The expression for the GCL coincides with that derived in [12] for the finite volume method. In the following, we present the conditions that the GCL imposes on the temporal integration. The derivation follows that in [12].

As shown in [12], the grid velocity has to be computed as follows

$$\vec{b} = \frac{\vec{x}^{n+1} - \vec{x}^n}{\Delta t}. \tag{16}$$

If we substitute Eq. (16) in Eq. (15), the expression $\int_{\partial S_T} \vec{b}\cdot\vec{n}\,\mathrm{d}\Gamma$ is linear in time. The time integral of Eq. (15) is then computed exactly using the midpoint rule, i.e. with geometrical quantities at $t^{n+\frac{1}{2}}$. This gives exactly the area swept by the boundary and satisfies the GCL condition as expressed by Eq. (15).

In summary, the GCL derived herein shows that for two-dimensional problems, the integrand of $\int_{t^n}^{t^{n+1}} \int_{S_T} \frac{\partial}{\partial x_k}(F_k - Ub_k)\,\mathrm{d}\Omega\,\mathrm{d}t = \int_{t^n}^{t^{n+1}} \Phi^T\,\mathrm{d}t$ in Eq. (10) must be evaluated at the midpoint configuration. This means that the cell fluctuation Φ^T must be evaluated with the quantities in between two time-steps, i.e. at $t^{n+\frac{1}{2}}$. This holds for nodal positions (hence areas and normals) as well as for nodal grid velocities. The integral must be computed as follows:

$$\begin{aligned}
\int_{t^n}^{t^{n+1}} \Phi^T(U,\vec{x},\vec{b})\,\mathrm{d}t &= \Delta t \Phi^T(U,\vec{x}^{n+\frac{1}{2}},\vec{b}^{n+\frac{1}{2}}) \\
\vec{x}^{n+\frac{1}{2}} &= \frac{\vec{x}^n + \vec{x}^{n+1}}{2} \\
\vec{b}^{n+\frac{1}{2}} &= \frac{\vec{x}^{n+1} - \vec{x}^n}{\Delta t}.
\end{aligned} \tag{17}$$

3.3. Conservative linearization on moving meshes

For the residual distribution discretization a conservative linearization is necessary to evaluate the different terms of the cell fluctuation. For the Euler equations the cell fluctuation in a triangle on a moving domain is computed from Eq. (9) as follows

$$\Phi^T = \int_{S_T} \vec{\nabla}\cdot\vec{F}\,\mathrm{d}\Omega - \int_{S_T} \vec{\nabla}\cdot(\vec{b}U)\,\mathrm{d}\Omega = \oint_{\partial S_T} \vec{F}\cdot\vec{n}\,\mathrm{d}\Gamma - \oint_{\partial S_T} U\vec{b}\cdot\vec{n}\,\mathrm{d}\Gamma. \tag{18}$$

These two integrals have to be evaluated such that conservation is guaranteed, i.e. that for a summation over all cells the fluxes at cell interfaces cancel out. The two integrands have different properties, hence we apply a different conservative linearization to each of them, making use of different assumptions and different notations for the gradient of U:

- For the first integral we use the Roe-linearization [13] assuming a linear variation of the Roe-parameter vector $Z = \sqrt{\rho}(1,u,v,H)^\tau$ over the element and denote the gradient of U by $\widehat{\nabla U}$.

The vector of flux Jacobians $\vec{A} = \partial\vec{F}/\partial U$, which is needed in the residual distribution schemes (see below), is evaluated at the average state of Z.

- For the second integral we assume a linear variation of U and $\vec{b}$ in space and denote the gradient of U by $\widehat{\vec{\nabla} U}$ and the divergence of the grid velocity by $\widehat{\vec{\nabla}\cdot\vec{b}}$.

For the evaluation of these integrals, the conservative linearization is then

$$\oint_{\partial S_T} \vec{F}\cdot\vec{n}\,\mathrm{d}\Gamma = \int_{S_T} \vec{\nabla}\cdot\vec{F}\,\mathrm{d}\Omega = \int_{S_T} \vec{A}\cdot\vec{\nabla}U\,\mathrm{d}\Omega \equiv \vec{A}(\bar{Z})\cdot\widehat{\vec{\nabla}U}S_T, \tag{19}$$

$$\begin{aligned}\oint_{\partial S_T} U\vec{b}\cdot\vec{n}\,\mathrm{d}\Gamma &= \int_{S_T} \vec{\nabla}\cdot(\vec{b}U)\,\mathrm{d}\Omega = \int_{S_T} \left(\vec{b}\cdot\vec{\nabla}U + U\vec{\nabla}\cdot\vec{b}\right)\mathrm{d}\Omega \\ &\equiv \left(\bar{\vec{b}}\cdot\widehat{\vec{\nabla}U} + \bar{U}\,\widehat{\vec{\nabla}\cdot\vec{b}}\right)S_T,\end{aligned} \tag{20}$$

where the overbar denotes the average state over the triangle. These expressions for the integrals are exact under the respective assumptions. The above assumptions ensure the conservation property even for a general flow that does not satisfy either of those two assumptions because the derived discretization formulas are exact contour integrals. For flows that do satisfy one of the assumptions the respective integral will be conservative and exact; for flows that do not satisfy either of the assumptions the integrals will still be conservative, but not exact.

The fluctuation in a triangle on a moving domain is computed from Eq. (18) using the expressions from Eqs. (19) and (20) and is written

$$\Phi^T = \left(\left[\vec{A}(\bar{Z}) - \bar{\vec{b}}I\right]\cdot\widehat{\vec{\nabla}U}\right)S_T + \left(\bar{\vec{b}}\cdot\left[\widehat{\vec{\nabla}U} - \widehat{\vec{\nabla}U}\right] - \bar{U}\,\widehat{\vec{\nabla}\cdot\vec{b}}\right)S_T, \tag{21}$$

whereas for a fixed mesh the fluctuation is simply calculated by $\Phi^T = (\vec{A}(\bar{Z})\cdot\widehat{\vec{\nabla}U})S_T$. For the computation of the cell residual in upwind residual distribution schemes on moving domains the velocity relative to the grid is needed. Therefore we have included in the convection term of Eq. (21) the grid speed, i.e. we have to subtract and add the term $(\bar{\vec{b}}I\cdot\widehat{\vec{\nabla}U}S_T)$. Together with the term $(\bar{\vec{b}}\cdot\widehat{\vec{\nabla}U}S_T)$ coming from Eq. (20), this gives an expression proportional to the difference of two gradients of U evaluated under different assumptions. This expression is zero for uniform flow, for non-uniform flow its influence is small [11]. We refer to this term as "conservation correction".

The term $(\bar{U}\,\widehat{\vec{\nabla}\cdot\vec{b}}S_T)$ in Eq. (21) is the geometrical source term proportional to the divergence of the grid velocity. This term is zero for rigidly moving meshes, i.e. when $\widehat{\vec{\nabla}\cdot\vec{b}} = 0$, but is of considerable importance when dealing with deformable meshes.

The convective term is distributed with the matrix of distribution coefficients $|\mathbf{B}_i^T$ of the particular residual distribution scheme, and the source term is distributed equally to the nodes by $\frac{1}{3}$ to satisfy the GCL. We distribute the conservation correction in the same way as the geometrical source term.

With the residual Φ_i^T from triangle T distributed to node i

$$\Phi_i^T = |\mathbf{B}_i^T\left(\left[\vec{A}(\bar{Z}) - \vec{\bar{b}}I\right] \cdot \widehat{\vec{\nabla}U}\right)S_T + \frac{1}{3}\left(\vec{\bar{b}} \cdot \left[\widehat{\vec{\nabla}U} - \widehat{\widehat{\vec{\nabla}U}}\right]\right)S_T - \frac{1}{3}\left(\bar{U}\,\widehat{\widehat{\vec{\nabla}\cdot\vec{b}}}\right)S_T, \tag{22}$$

the residual distribution discretization then reads

$$\frac{S_i^{n+1}U_i^{n+1} - S_i^n U_i^n}{\Delta t} = -\sum_T \Phi_i^T. \tag{23}$$

As shown in this section, the cell fluctuation reveals for deforming meshes a geometrical source term which is not of a physical origin, but is only due to the deformation of the mesh. Consequently this term has to be accounted for, because otherwise the physics of the flow would be changed. The different terms of the cell fluctuation Φ^T are to be distributed such that the GCL is fulfilled.

4. Transonic flow over an oscillating NACA 0012 airfoil

4.1. Presentation of the testcase

A standard NACA 0012 airfoil is pitching harmonically around the quarter chord. The upstream Mach number is 0.755 and the mean angle of incidence is 0.016°. The airfoil performs a sinusoidal pitching motion with an amplitude of 2.51°:

$$\alpha = 0.016° + 2.51° \sin(2kt), \tag{24}$$

where k is the reduced frequency ω of oscillation with respect to the half-chord:

$$k = \frac{\omega c}{2V_{\text{inf}}} = 0.0814. \tag{25}$$

In Eq. (25), c denotes the chord length and V_{inf} the upstream flow velocity. This oscillatory motion of the airfoil is adopted for the grid, i.e. the grid oscillates rigidly with the same amplitude and frequency as the airfoil around the quarter chord. Fig. 1 shows a section of the unstructured 2355

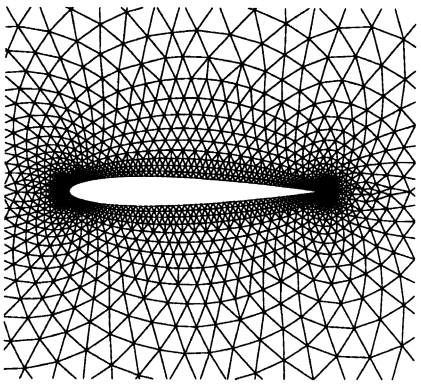

Fig. 1. Partial view of unstructured grid with 2355 nodes.

nodes grid that was used in the simulation. The grid extends over a distance of 20 chords towards the far field where the upstream values are imposed as boundary conditions. On the airfoil surface an inviscid wall boundary condition is applied.

The numerical scheme used in the present explicit computation is the PSI-scheme [7]. In combination with a lumped mass matrix it is only first-order accurate for unsteady computations [9]. The present testcase can be considered as a quasi-steady problem because the time-step is very small in comparison with the characteristic time scale of the airfoil oscillation. For steady problems the PSI-scheme is second-order accurate, thus the solution of this quasi-steady process is almost second-order.

4.2. Results

Starting from the steady-state flow field at mean incidence, the sinusoidal pitching motion is started at time zero. Three cycles of oscillations are computed and periodicity is achieved within the third cycle (Fig. 2). This figure shows the evolution of the lift coefficient as a function of the pitch angle during three cycles of oscillation.

The results are presented for the third cycle of oscillation. They are given in terms of Mach number isolines and wall pressure coefficient distributions at instantaneous times. The Mach number isolines at two instantaneous times during the third cycle are presented in Fig. 3a and b where the symbol ↓ indicates the downstroke motion of the airfoil. In Fig. 4a and b the instantaneous distribution of the wall pressure coefficient is shown at the same instants as the Mach number isolines.

The whole sequence of instantaneous images is given in [11] where it appears that the most obvious physical effect is the delay of the shock motion with respect to the airfoil oscillation.

We have compared our numerical results with those in [14] and with experimental data in [15]. Generally, a good agreement has been found between our computation and both the reference computation [14] and experimental data [15].

For this testcase of the oscillating airfoil, the relevance of the conservation correction (Eq. (22)) has also been investigated [11]. It is a suitable testcase for this purpose as there are regions with

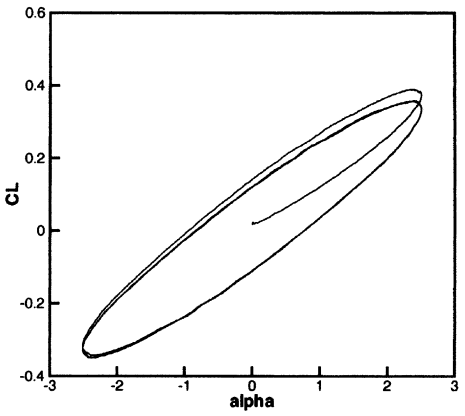

Fig. 2. Computed lift coefficient during three cycles.

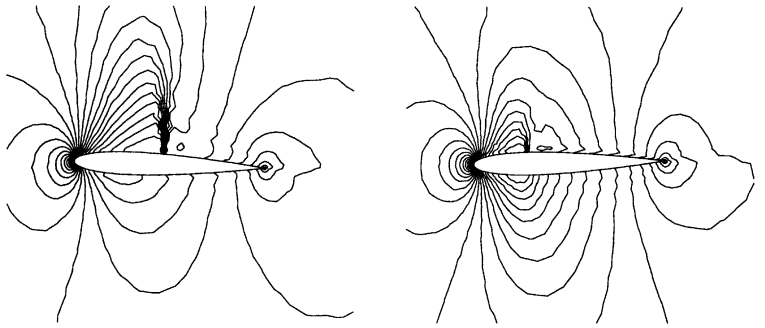

a: $2kt = 127^{\circ}, \alpha = 2.01^{\circ}, \downarrow$ b: $2kt = 210^{\circ}, \alpha = -1.25^{\circ}, \downarrow$

Fig. 3. Mach number isolines during the third cycle for two instants.

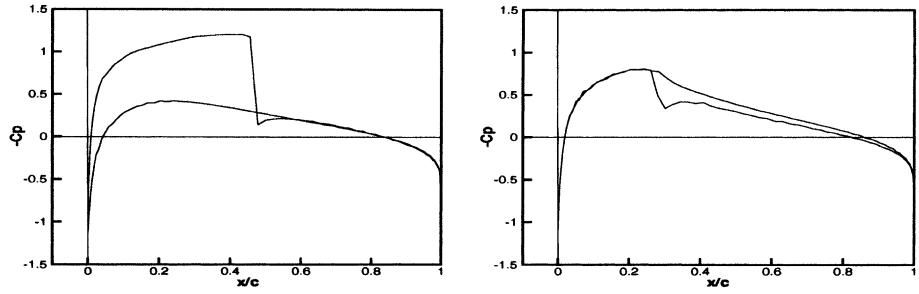

a: $2kt = 127^{\circ}, \alpha = 2.01^{\circ}, \downarrow$ b: $2kt = 210^{\circ}, \alpha = -1.25^{\circ}, \downarrow$

Fig. 4. Pressure coefficient distributions during the third cycle for two instants.

strong gradients. The influence of this conservation correction has been found to be negligibly small in this case, which is somewhat surprising.

5. Vortex convected in an inviscid low speed free-stream

5.1. Presentation of the testcase

This testcase is used to validate the algorithm also on deforming meshes and to investigate the influence of the geometrical source term.

The initial vortex is defined by an angular velocity u_θ given by the following analytical form

$$\frac{u_\theta}{V_{\max}} = \begin{cases} \dfrac{r}{a_0} & \text{if } r \leqslant a_0 \\ \exp\left(-\dfrac{(r-a_0)^2}{\Omega} \right) & \text{if } r > a_0 \end{cases} \tag{26}$$

with $V_{\max} = 0.9047$ and $\Omega = 0.03$. The core radius a_0 is equal to $0.12L$, where L is a reference length. The pressure and density distributions are obtained from the radial momentum and energy equations. The pressure reaches a minimum at the core of the vortex and is equal to $0.951p_{\inf}$, where $p_{\inf}$ denotes the pressure in the far field. For the parameter settings we refer to [16].

The stationary vortex is superimposed on a low speed uniform flow with a Mach number of 0.2. Thus, the velocity components of both vortex and uniform flow sum up, whereas the pressure and density distributions remain the same as for the stationary vortex.

In theory, all wave modes should travel with the same speed and therefore preserve the integrity of the vortex. Especially the sharp pressure dip at the center of the vortex should be preserved. In practice, the core pressure rises during the movement of the vortex due to the dissipative effects of the numerical scheme employed. We investigate how different ways of grid movement affect the final shape of the vortex. Comparisons are made to validate the implementation of rigidly moving and deforming meshes for the Euler equations.

The computational domain extends over $[-0.6; 2.1] \times [-0.6; 0.6]$ and an unstructured grid with 90×40 nodes is used. Fig. 5 shows the initial vortex on the grid. The vortex travels a distance of $1.5L$. We employ subsonic inlet and subsonic outlet boundary conditions, upper and lower wall are specified as inviscid walls.

The numerical scheme used in these computations is the LDA-scheme [7].

5.2. Results

A reference computation has been carried out on a fixed mesh and three computations have been performed for a mesh moving in the horizontal direction. The different ways of grid movement are the following:

- a grid moving rigidly with 80% of the convection speed,
- a grid expanding in the horizontal direction with an expansion factor of 1.5 (ratio of final and initial grid length),
- a combination of a moving (50% of the convection speed) and expanding grid (expansion factor of 1.5).

In Fig. 6, we compare pressure distributions along a line that crosses the vortex in its center. The final core pressure has increased in comparison with the initial one due to numerical dissipation.

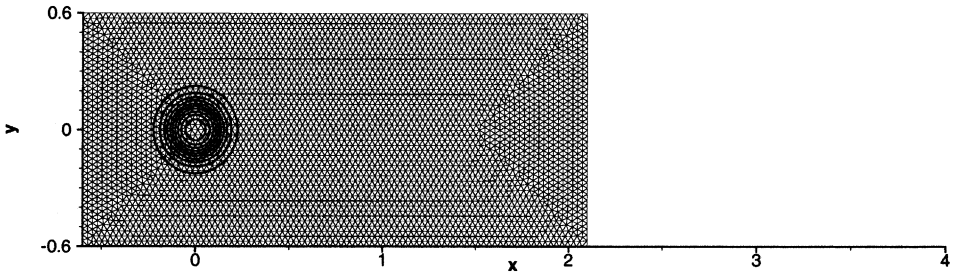

Fig. 5. Convected vortex: initial solution in terms of isobar lines.

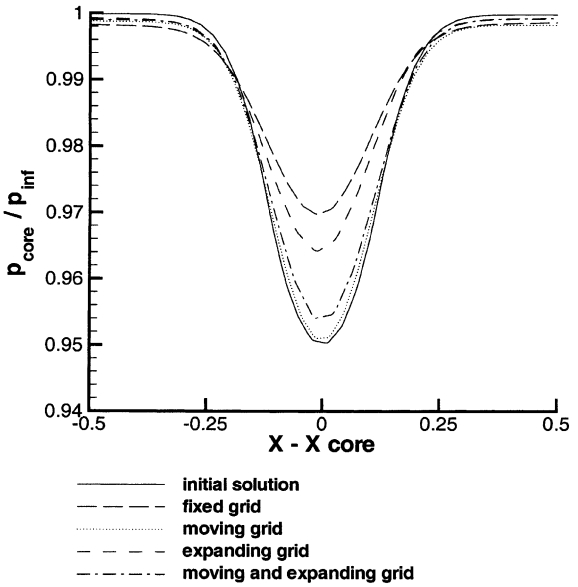

Fig. 6. Pressure distribution along a line crossing the vortex in the center.

It is obvious that the pressure distribution and the sharp pressure dip at the core for a vortex on a grid moving with 80% of the convection speed are close to the initial distribution because the vortex crosses fewer cell boundaries. For a grid moving with exactly the convection speed the initial solution is almost perfectly preserved. The pressure distribution for an expanding grid is closer to the initial pressure distribution than for the fixed one although the grid becomes coarser. The reason is that the expansion takes place in the direction of the vortex movement and again the vortex crosses fewer cell boundaries. However, the pressure dip is not as sharp as on a rigidly moving mesh. For the combination of moving (50% of the convection speed) and expanding grid (expansion factor of 1.5) the final solution is between the solution for a purely moving grid and the one for a purely expanding grid. These results are consistent.

We have used this testcase also to investigate the influence of the source term on the solution. For this purpose a computation on an expanding mesh (expansion factor of 1.5) is done neglecting the source term in the cell fluctuation. The integrity of the vortex is destroyed already after a quarter of the travel distance and the computation fails. As expected, it appears thus essential to take the source term into account when it is not zero.

6. Discussion and conclusions

An ALE formulation has been derived for the residual distribution method on moving meshes. The system of Euler equations has been discretized on moving meshes, and in case of deforming meshes a geometrical source term has to be taken into account. By means of a conservative linearization the conservation property of the discretized equations is guaranteed. This leads to an additional term in the cell fluctuation which we call conservation correction.

The ALE scheme is designed to satisfy the GCL. This requires evaluating the cell fluctuation Φ^T at $t^{n+\frac{1}{2}}$ and distributing the geometrical source term to the nodes using the same mass matrix as that used for the time discretization.

We have computed the testcase of the flow around a transonic oscillating airfoil employing a rigidly moving mesh. The results show good agreement with reference data. The considerable influence of the geometrical source term on the solution has been demonstrated for the testcase of the convected vortex employing a deforming mesh.

The ALE formulation works properly to compute flow problems with moving boundaries where the movement of the mesh becomes necessary. Future research will extend to other problems with moving boundaries such as aeroelasticity where the grid motion is no longer prescribed as in the testcases of this work, but is defined by fluid-structure interaction.

Acknowledgements

This research has been carried out during the Diploma Course 1999/2000 at the von Karman Institute, Sint-Genesius-Rode (Belgium). Furthermore, I would like to thank Prof. R. de Borst, TU Delft for the constructive discussions about this subject.

References

[1] Demirdzić I, Perić M. Finite volume method for prediction of fluid flow in arbitrarily shaped domains with moving boundaries. Int J Numer Meth Fluids 1990;10:771–90.
[2] Allen CB. Adaptation by grid motion for unsteady Euler aerofoil flows. In: Paper Presented at the AGARD FDP Symposium on Progress and Challenges in CFD Methods and Algorithms, held in Seville, Spain from 2–5 October 1995, published in CP-578, 1995.
[3] Batina JT. Unsteady Euler airfoil solutions using unstructured dynamic meshes. AIAA Paper No. 89-0115; January 1989.
[4] Rausch RD, Batina JT, Yang HTY. Euler flutter analysis of airfoils using unstructured dynamic meshes. J Aircraft 1989;27(5):436–43.
[5] Deconinck H, Sermeus K, Abgrall R. Status of multidimensional upwind residual distribution schemes and applications in aeronautics. AIAA Paper No 2000-2328; 2000.
[6] Paillère H. Multidimensional upwind residual distribution schemes for the Euler and Navier–Stokes equations on unstructured grids, PhD thesis, Université Libre de Bruxelles; June 1995.
[7] van der Weide E, Deconinck H. Matrix distribution schemes for the system of Euler equations, Euler and Navier–Stokes solvers using multi-dimensional upwind-schemes and multigrid acceleration. In: Notes on Numerical Fluid Mechanics, vol. 57. Braunschweig: Vieweg; 1997.
[8] Bonfiglioli A, Deconinck H. Multidimensional upwind schemes for the 3-D Euler equations on unstructured meshes, Euler and Navier–Stokes solvers using multi-dimensional upwind-schemes and multigrid acceleration. In: Notes on Numerical Fluid Mechanics, vol. 57. Braunschweig: Vieweg; 1997.
[9] Maerz J. Improving time accuracy for residual distribution schemes, Project report, von Karman Institute for Fluid Dynamics; June 1996.
[10] Ricchiuto M. Time accurate solution of hyperbolic partial differential equations using FCT and residual distribution, Stagiaire report, von Karman Institute for Fluid Dynamics; September 1999.
[11] Michler C. Development of an arbitrary Lagrangian Eulerian formulation for unsteady flow computations on moving meshes using residual distribution schemes, Project report, von Karman Institute for Fluid Dynamics; June 2000.

[12] Lesoinne M, Farhat C. Geometric conservation laws for aeroelastic computations using unstructured dynamic meshes. AIAA Paper No 95-1709-CP; 1995.
[13] Roe PL. Approximate Riemann solvers, parameter vectors and difference schemes. J Comput Phys 1981;43(2):357–72.
[14] Rogiest P. An implicit finite volume scheme for the computation of unsteady compressible flows on multi-block structured grids: application to aeroelastic problems, PhD thesis, Université de Liège; April 1997.
[15] Landon RH. NACA0012. Oscillatory and transient pitching, compendium of unsteady aerodynamic measurements, AGARD-R-702, AGARD, 1982.
[16] Broussard H. Unsteady flow computations on moving meshes using residual distribution schemes, Project report, von Karman Institute for Fluid Dynamics; June 1998.